

Redefining Fasciocutaneous Microanatomy: An Illustrated Review of Current Concepts and Their Clinical Correlates

Mohammad Suleman Bajwa, MBBS, MD^{1,2*}; Muhammad Omar Afzal, MBBS, FCPS¹; Ahmad Hussain, MBBS¹; Usman Khalid Farooq, MBBS, FCPS¹; Muhammad Mustehsan Bashir, MBBS, FCPS, MME, PhD¹; Farooq Shahzad, MBBS, FACS, FAAP³



¹Department of Plastic and Reconstructive Surgery & Mayo Burn Centre, Mayo Hospital, King Edward Medical University, Punjab, Pakistan

²Department of Surgery, Montefiore Medical Center, Albert Einstein College of Medicine, New York, USA

³Plastic and Reconstructive Surgical Service, Department of Surgery, Memorial Sloan Kettering Cancer Center, New York, USA

ABSTRACT

Emerging anatomical concepts challenge microsurgical dogma. The current anatomy of the skin and subcutaneous tissue was reviewed with the objective of challenging the existing understanding of fasciocutaneous microanatomy using an updated anatomical model. Numerical anatomical data were compiled and utilized to create an updated and scaled model, defining integumentary neuroarterial, venolymphatic, and connective tissue systems. Additionally, a second model detailing the neurovasculature of the head and neck is presented, illustrating the relations of perforator arteries. Microangiosomes, the strength of their connections, and their relation to dissection planes are described. Clinically relevant structures are outlined, along with general principles and regional variations. We explore the viability of dermal plexus flaps and their potential for engraftment through plexus-to-plexus apposition. A comparison is drawn between subdermal and deep-dermal plexi. Furthermore, the peculiarities of head and neck perfusion and lymphatic drainage are discussed. These models inform our approach to dissection planes, fluid injection depths, flap viability, neurotization, post-inflammatory hyperpigmentation, tissue engraftment, debulking, and head and neck lymphatic drainage. This illustrated review offers an updated understanding of fasciocutaneous microanatomy and how to safely utilize it.

INTRODUCTION

In the microsurgical era, the distinction between flaps and grafts has become blurred. The success of thin pure-skin flaps [1] and thick skin-fat composite grafts [2] reflects a growing command over microvascular anatomy. Nevertheless, some erroneous concepts persist that can jeopardize tissue viability and patient safety. Dermal plexus flaps are used to re-drape entire limbs [3–5], show a limited area of perfusion on perforator imaging [1], and often suffer marginal necrosis during excisional debulking [6,7]. Certain grafts become vascularized within 24 hours through direct anastomoses between remnant vessels [8]. These paradoxes expose the need to update our understanding of cutaneous microvasculature to better inform surgical practice.

This study aims to redefine current understanding of fasciocutaneous microanatomy by challenging prevalent concepts with an updated anatomical model. Specifically, it explores microangiosomes, compares the dermal plexi, and investigates head and neck perfusion and lymphatic drainage. The objective of this research is to enhance microsurgical techniques and improve patient outcomes by providing insight into the limitations of existing procedures across various clinical scenarios.

METHODS

To develop the primary model, we purposively retrieved articles on anatomy of each component of the integumentary system from PubMed (MEDLINE), Sco-

pus and Google Scholar from January 1970 to April 2023 (initial search conducted through December 2022). The keywords used include 'skin', 'cutaneous', 'integument', 'subcutaneous', 'microanatomy', 'microscopy', 'vasculature', 'artery', 'vein', 'lymphatic', 'perforator', 'perfusion', 'neuroanatomy', 'nerve', 'innervation', 'melanocyte', 'connective tissue', 'collagen', 'fascia', 'adipose', and 'fat'. Secondary retrieval was done using a citation-networking software (ResearchRabbit, Version 2.0, Human Intelligence Technologies, Incorporated) until we achieved concept saturation. We only included studies on human skin and/or subcutaneous anatomy, which observed at least 5 tissue samples. We excluded studies which were simulation-based, discussed only post-surgical imaging, reported unoriginal concepts, or those deemed not surgically relevant, as determined by consensus between two reviewers. In cases of ambiguity, the senior reviewer's decision was solicited. Objective data and images were used to prepare a scale model. In our reporting, we emphasized the structure of microangiosomes, the strength of plexus connections, and their relation to dissection planes. In the discussion, we explore the role of the updated model in clarifying our understanding of aspects of microsurgery, specifically dissection planes, injection depths, flap viability, neurotization, post-inflammatory hyperpigmentation, tissue engraftment, debulking, and head and neck lymphatic drainage.

RESULTS

To prepare the primary model (Figure 1), our literature review comprised 22 original articles and reviews, focusing on the anatomy of connective tissue

[9,10], the adipofascial system [11–14], lymphatics [10,15], veins [10], special organs [16], and arteries along with their accompanying nerves [1,10,17–29]. Among these, 9 were most essential in preparing the final model [9–11,14,15,18,21,24,27,29]. Measurements of structures are compiled in Table 1. For clarity, the dermal papillae are depicted as wider, while the deeper plexi have not been fully elaborated. Regional variations are summarized in Table 2 [11,30]. Individual systems are detailed below, and their surgical implications are reviewed in the discussion section.

Melanocytic System

The basal layer of the epidermis houses melanocytes. These neural crest cells have a dermatomal distribution [31]. They are also found in hair bulbs, and perhaps in sebaceous glands [32]. Melanocyte density doubles in the rete ridges as compared to the inter-ridge area [33,34]. Thus, thicker grafts have exponentially more melanocytes.

Connective Tissue System

The mechanical properties of skin and its dissection planes are of surgical relevance. The epidermis (Figure 1 label #1) is of variable thickness (Table 2) [30]. The undulating dermo-epidermal interface contributes the most to skin shear-resistance [10]. This interface is flat in extremes of age, contributing to easy bruising. Additionally, aged skin exhibits dermal thinning from keratinocyte apoptosis and senescence, fewer blood vessels, and larger, albeit hypofunctional, sebaceous glands [35]. Photoaging independently reduces shear-resistance and contributes to dermal thickness changes. Photoaging affects sun-protected skin (e.g., torso) more as compared to sun-exposed skin (e.g., forearm or calf) [36]. Integumentary ligaments anchor rete ridges to deeper layers (Figure 1 label #8). These 'retaining ligaments' are prominent in the unaged face, and in patients with early Dupuytren's hand contracture [11,37,38]. They transmit contractions of superficial muscles to the skin, while protecting the vessels.

There are three distinct densities of the dermal extracellular matrix [9]. The superficial (papillary) dermis (Figure 1 label #7) is collagen-and-elastin-rare. The middle (upper reticular) dermis is the thickest layer and is uniformly dense (Figure 1 label #9). The deepest 0.18 mm of the reticular dermis (Figure 1 label #11) is also rare. The dense middle dermis makes intradermal injection difficult. It reflects injected fluid back up, raising the papillary dermal plane [39]. This layer may act as a barrier to the transmission of infiltrated fluids (anesthetics, fillers, etc.) across planes, whether injected intradermally or subdermally [40].

Regional variations in connective tissue lead to anisotropy in skin tension lines [41,42]. Collagen-elastin interplay accounts for skin biomechanical properties, like non-linear deformation, anisotropy, and viscoelasticity [43]. Collagen provides an excellent surface for early fibrin-mediated adherence of wound edges, and for late biointegration [44]. Thicker grafts are less likely to contract [45,46], and their scar sheet may enhance tissue strength [47].

Adipose Tissue

Subcutaneous white adipose tissue comprises the superficial/protective and deep/lubricant adipofascial systems [11]. The superficial system consists of densely packed adipocytes that are tethered between the superficial fascia and dermal integumentary ligaments by the honeycomb fascia (Figure 1 label #12, 13). It has a cushioning effect. The deep system has loose striated fascia, which allows planes to glide smoothly (Figure 1 label #15, 16). These systems are phenotypically distinct. The superficial system serves a fat metabolism function, while the deep system is pro-inflammatory [14]. The adipofascial system lends pliability to skin-fat composite grafts [2]. Their distribution differs across the body (Table 2).

Dense aggregates of adipocytes form secondary microlobules. These receive end-arterial supply (Figure 1 label #12). Superficial fat arteries are smaller, albeit more numerous, than those in deep fat [14]. Deep fat receives additional perfusion from descending branches of deep dermal and subdermal plexi (Figure 1 label #56) [14,18]. Our clinical observation is that fat necrosis predominantly involves deep fat. While it is the better-perfused layer, cells in the deep

fat overexpress cell-death genes [14].

Microlobules receive central end-arteries and are peripherally drained along septae (Figure 1 label #33). Arterial pathology primarily affects the lobule (lobular panniculitis), and venous disease affects the septal and paraseptal areas (septal panniculitis) [12]. In degloving trauma, the shearing action severs perforators ascending to the deep fat (Figure 1 label #57) [48].

In some regions, like the thigh, there are multiple adipofascial layers [13]. In obesity, adipose expansion and fibrosis lead to the formation of more adipofascial layers, separated by pseudo-superficial fascia (thickened honeycomb fascia) (Figure 1 label #13) [49]. Deep fat predominates in abdominal obesity (Table 2).

Venolymphatic System

Till recently, it was assumed that there exist subpapillary venous, arterial, lymphatic, and nervous plexi [10,23,27]. High-resolution episcopic microscopy studies confirm the presence of a subpapillary venous plexus and the absence of an arterial one (Figure 1 label #24, 61) [21,24,25]. Relevant venular physiologic phenomena include the venoarterial reflex (venous distension prompts systemic vasoconstriction), the venuloarterial reflex (venular distension prompts regional arteriolar constriction), and the Bayliss effect (venular distention prompts mural venous constriction) [50].

Pre-nodal lymphatics consist of 4 distinct types of channels (Figure 1 labels #18–22) [15]. They traverse collagen-rare planes, into which large proteins readily drain (Figure 1 label #19). Tissue edema pulls tethers that maintain lymphatic channel patency and open drainage pores. Like veins, their semilunar valves emerge in the deeper dermis (Figure 1 label #21). Lymphatics do not directly drain fat (Figure 1 label #22), hence the necessity of burn escharotomy. Veins and lymphatics are closely related [10]. Cellular plasticity, lymph node shunts, and dissection studies suggest the natural occurrence of macrovascular lymphatic/blood linkages [15,51].

In the head and neck, lymphatic drainage is complex. Collecting ducts from a single site drain to multiple different nodal basins [52,53]. These ducts travel laterally, towards the scalp and lateral face and neck [53,54]. Injury to these ducts results in prolonged edema, which requires about 3 weeks for repair [55]. The superficial and deep lymphatic system sandwich the superficial musculoaponeurotic system (SMAS) [54]. Valveless interconnections run between the two. Surgical insult to either system can result in prolonged edema [54].

Neuroarterial System

Cutaneous nerves and arteries are closely related [10,22]. Dermal sensory nerve bundles arborize like arteries (Figure 1 label #62) [25,29]. Superficial fascial and subdermal neurovascular 'freeways' parallel specific cutaneous nerves [56]. These vascular axes begin with arteries (e.g., descending genicular artery), distally make true anastomoses with long axial perforators (e.g., from the posterior tibial artery), and run in parallel to specific large nerves (e.g., saphenous nerve) [22,56]. These nerves are slightly apart from the arteries and can be separated. However, their inclusion in flaps increases the chances of preserving the vascular axis. Along cutaneous nerves, even choke vessels are relatively large [56].

The papillary dermis has a rich capillary supply, though no true plexus exists here [10,23]. Papillary perfusion is thermoregulated. In the reticular dermis, flow is metabolism/hypoxia-mediated [40,41].

Contrary to previous descriptions [1,18], the deep dermal plexus is distinct from the subdermal plexus (Figure 1 labels #53 and 54) [9,21,24]. It is random patterned, unlike the more axial subdermal plexus [18,27]. Its ascending vessels perfuse small 'microangiosomes' (see Table 1 for areas) [1]. Microangiosomes do not form any plexus, only a few insignificant anastomoses (Figure 1 labels #50–52) [21,24]. At the border of adjacent subdermal angiosomes, neighboring microangiosomes have slightly larger anastomoses and territories (see Table 1) [24].

Subdermal angiosomes are demarcated by 'choke vessels.' These are small-caliber regulatory vessels. They dilate (arteriogenesis) under the influence of vasodilators, high flow, and vascular delay [22,43]. Angiosomes hardly

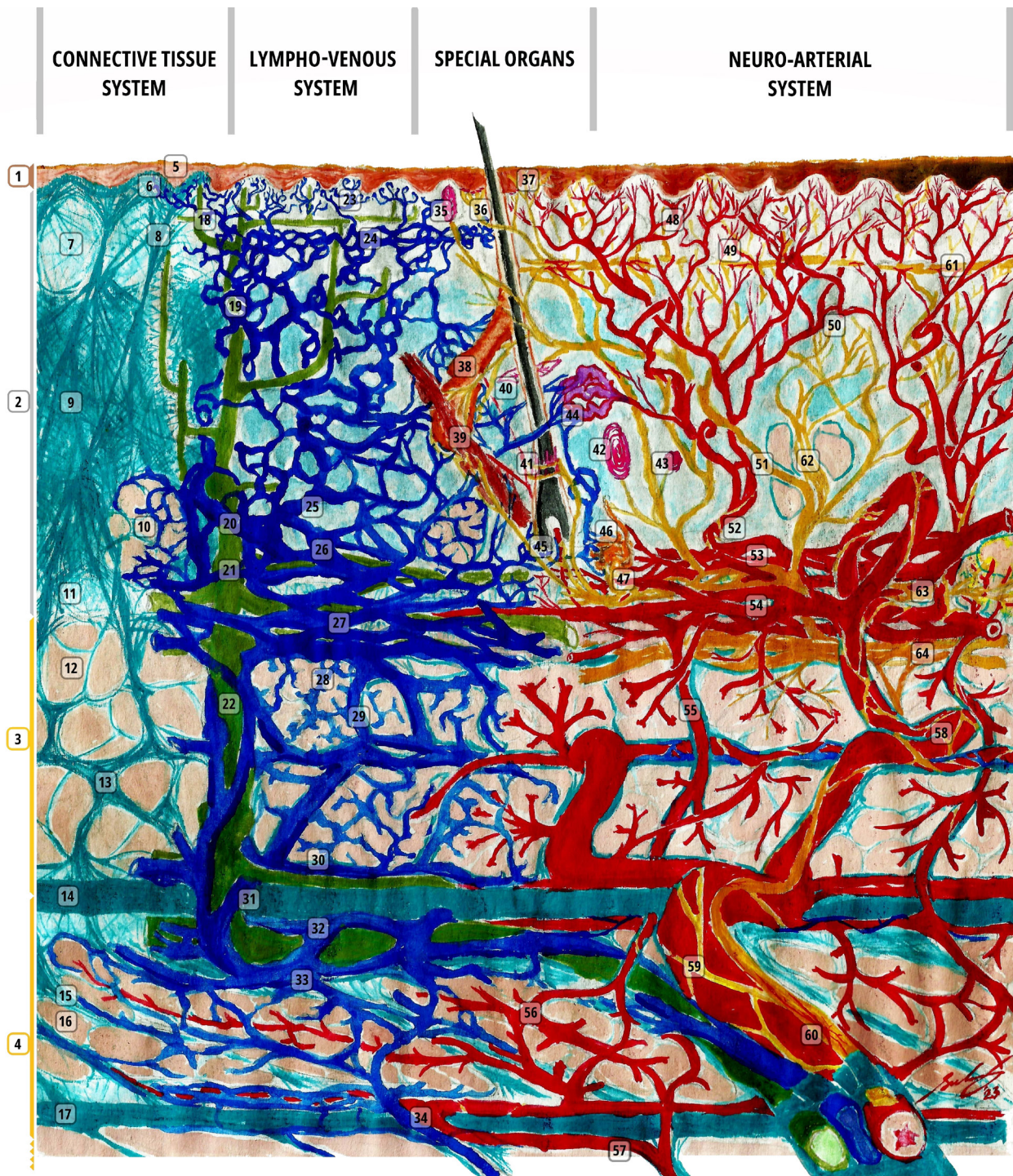


Figure 1. A scale representation of the human integumentary system (30:1, with a hair shaft width as a 70 µm reference). Connective tissue (1-17, colored in cyan for collagen fibers and beige for adipose): 1, epidermis; 2, dermis; 3, protective adipofascial system; 4, lubricant adipofascial system; 5, rete peg; 6, dermal papilla; 7, papillary dermis (collagen rare); 8, integumentary ligament; 9, reticular/deep-dermis (collagen-dense layer); 10, adipose tissue in dermis; 11, reticular/deep-dermis (collagen-rare layer); 12, cuboid fat; 13, honeycomb fascia; 14, superficial membranous fascia; 15, striated fascia; 16, flat fat; 17, deep membranous fascia. Lymphatics (18-22, colored in green): 18, initial lymphatic (open-ended, avascular channel); 19, pre-collector lymphatic (has valves); 20, lymphagion (channel between valves) of a collector lymphatic (has circumferential contractile cells); 21, semilunar valve; 22, pre-nodal lymphatic trunk. Veins (23-34, colored in deep blue): 23, venule; 24, subpapillary venous plexus; 25, semilunar valve (start in deep dermal layer); 26, deep dermal plexus; 27, subdermal plexus; 28, peripheral tributary; 29, interlobular septal vein; 30, suprafascial plexus; 31, superficial fascial perforator; 32, subfascial plexus; 33, venous tributaries (peripheral/septal); 34, deep fascial perforators. Special organs (35-47): 35, Meissner corpuscle; 36, Merkel disc; 37, free nerve endings; 38, sebaceous gland; 39, arrector pili muscle; 40, Ruffini ending; 41, lanceolate-ending receptors; 42, Pacinian corpuscle; 43, Krause end bulb; 44, glomus body (closely related to 42); 45, hair bulb and hair-end nerve plexus; 46, eccrine sweat gland; 47, sudomotor plexus. Arteries (48-60, colored in red): 48, terminal dermal arteries giving off papillary capillaries; 49, epineural arterial complex; 50, inter-microangiosomal anastomosis (rare); 51, intra-microangiosomal anastomosis (rare); 52, 'central dermal' microangiosomal artery; 53, deep dermal plexus; 54, subdermal plexus; 55, descending adipofascial artery; 56, anastomoses of the deep fatty layer; 57, deep fascial perforators; 58, septal artery; 59, nervi arteriosum; 60, vasa nervosum. Nerves (61-64, colored in yellow): 61, subpapillary nerve plexus; 62, dermal nerve trunk (whose branches follow dermal arteries); 63, deep dermal plexus; 64, cutaneous nerve and anastomoses. This figure is an original creation by the first author, prepared for this publication.

Table 1. Dimensions Considered in Model Design¹

Location	Dimension	
Skin layers		
Epidermis	Overall: Approximately 150.0 µm deep Eyelid: 5.0–50.0 µm Volar finger: 420.0–673.0 µm Sole: 529.0–1377.0 µm	
Dermal papillae	170.0 µm wide	
Venous subpapillary plexus	300–400.0 µm deep to surface	
Hair shaft	Approximately 70.0 µm wide	
Dermis	2.0–5.0 mm deep	
Papillary dermis (collagen-rare)	Up to 773.6 µm deep to dermo-epidermal junction	
Reticular dermis (collagen-dense)	Situated between the collagen-rare layers	
Reticular dermis (collagen rare)	Up to 171.9 µm above the dermo-hypodermal interface	
Dermo-hypodermal junction*	2500.0–3500.0 µm deep to surface	
Adipocyte	Up to 100.0 µm wide	
Arterial system		
Pre and post capillary vessels	8.0–15.0 µm	
Papillary dermal vessels	17.0–22.0 µm	
Initial (papillary) lymphatic vessel	60.0 µm	
Adjacent measurements ²	Within subdermal angiosome	Between subdermal angiosomes ³
Arterio-arterial anastomoses ⁴	17.0–40.0 µm	17.9–79.4 µm
‘Central dermal’ microangiosomal artery ⁵	29.3–89.5 µm	27.2–81.8 µm
Dermo-hypodermal artery	55.4–153.3 µm	58.0–189.2 µm
Number of microangiosomal arteries ⁶	0.0–3.0	0.0–3.0
Number of arterio-arterial anastomoses ⁶	0.0–4.0	1.0–5.0
Microangiosome area	1.6 ± 1.3 mm ²	1.8 ± 1.6 mm ²
Microangiosomal overlap area	0.9 ± 0.9 mm ²	0.7 ± 0.8 mm ²
Adipose septal artery	250.0–500.0 µm	
Arteriole to adipose secondary microlobule	100.0–300.0 µm	
Dermal-flap perfusion area (single pure-skin perforator)	29.0 ± 18.0 cm ² (3.0–60.0 cm ²)	
Dermal-flap perfusion area (double pure-skin perforators)	43.0 ± 20.0 cm ² (16.0–90.0 cm ²)	
Dermal-flap perfusion area (triple pure-skin perforators)	46.0 ± 33.0 cm ² (23.0–90.0 cm ²)	

¹The table is formulated based on references 1, 9, 11, 12, and 66.

²The measurements adjacent to each other represent values within an angiosome (on the left) and those between angiosomes (on the right). The region between subdermal angiosomes seems to feature more numerous microangiosomal anastomoses and larger microangiosomal areas.

³Measurement taken in region between neighboring subdermal angiosomes. This region appears to have wider anastomoses and broader microangiosome areas.

⁴May be found at any depth within the dermis, including anastomoses between and within microangiosomes.

⁵Emerges from deep dermis at intervals of 1.5 mm.

⁶In a cuboid data volume with base area of 5.76 mm².

cross scar lines [17,20,57].

Deep fascial perforators are consistently found within anchoring/fixed connective tissue planes, like at the modiolus. Here, perforators are protected from shear stress and have a shorter course to the skin. Perforators may be cutaneous, septocutaneous, or musculocutaneous. They respectively supply axial, fasciocutaneous, and random-pattern flaps, though there are many exceptions to this nomenclature [43]. Perforator diameter relates to tissue mobility and laxity [22]. In the face, arterial perforators are larger and closer to veins caudally compared to cranially [58].

Head and neck neuroanatomy is complex. Perforators mostly arise from the facial, superficial temporal, and supratrochlear arteries, along fascial planes [38,59]. There are true midline anastomoses in the lips [59], but choke anastomoses across the forehead [60]. Dense arterial plexi exist deep to, within, and superficial to the SMAS. The subdermal plexus is particularly rich in the

‘blush regions’ (malar area and anterior neck) [60]. Veins travel distant from arteries in the nasolabial area, forehead, and scalp [61]. Recent studies suggest glabellar flaps can include longer vessels (paracentral artery and central artery) and larger veins (central vein) than paramedian flaps (based on the supratrochlear artery) [62–64]. However, these central arteries may be absent in some patients. There exist communications between midfacial sensory (infraorbital) and motor (facial) nerve trunks, located around 16 mm lateral and 6 mm superior to the alar rim (Figure 2) [65]. This region may provide an alternate pathway for sensory and motor neurotization, i.e., a ‘babysitter nerve’, and should be safeguarded. Relations between facial perforators and surrounding neurovasculature are understudied compared to limbs. Figure 2 depicts the current anatomy of facial perforators and their relation to sub-SMAS neurovasculature.

Special Organs

Table 2. Regional Variations¹

Structure	Location
Verrucous skin	Eyelid, knee, and elbow
Flat dermal papillae	Limbs, eyelids, and skin in age extremes
Dermis	Thick on back Thin on anterior trunk and limbs
Dermo-hypodermal interface	Well-defined in trunk Poorly defined in limbs and lips
Hypodermis	Thick in cheek and labia majora Thin in forehead, eyelid, penile shaft, and labia minora
Bilayer fat ²	Face, abdomen, and back
Cuboid fat predominant	Pressure areas: palms, posterior shoulders, back, buttocks, thighs, and soles Accompanied by prominent anchoring fascia in skin creases, fossae, and cleavage sites
Flat fat predominant	Forearm, leg, and obese abdomen

¹The table is formulated based on references 11 and 30.

²Bi-layered fat consists of a superficial adipofascial system (superficial cuboid fat with honeycomb fascia) and a deep adipofascial system (flat fat with striated fascia).

The special organs in the skin (Figure 1 labels #35–47) are well-reviewed by Me-tze et al. [16]. Glomus bodies (Figure 1 label #44) shunt deep dermal arteries into veins. They are present in distal extremities alongside Pacinian corpuscles (Figure 1 label #42). This suggests that glomal perfusion is neuroregulated [16].

DISCUSSION

This study unveils the contemporary microanatomy of the integumentary system. The ensuing sections delve into its many microsurgical implications.

Dissection Planes

Surgical planes are often collagen-rare, allowing blunt dissection. Fluid from tissue edema, fasciitis pathogens, and injections travel along these planes. Arteries traverse them, but they still require delicate handling to avoid bleeding.

The deep-dermal plane, running within the dermo-hypodermal interface, begs description. There is no clear interface, especially in distal extremities (Figure 1 label #10 and Table 2). Indeed, full-thickness skin grafts often contain elements of both layers [27,47]. Horizontal vessels populate this wide region of deep dermis and subdermis [18,21,24,27]. This network can be subdivided into the deep dermal (Figure 1 label #53) and subdermal plexi (Figure 1 label #54). Separation requires meticulous fat dissection or hydrodissection through the deepest reticular dermis [1,2,9]. We believe this plane divides the plexi unequally, favoring the subdermal plexus. Angiography reveals the insufficiency of the deep dermal plexus [1]. Some surgeons propose that vertical perforators run between the subdermal and deep-dermal plexi [2]. However, imaging reveals these two plexi are continuous, horizontal, and lack any intervening solid membrane [9,18,24]. The vertical vessels observed are likely plexus vessels displaced by hydrodissection or descending adipofascial branches of these plexi (Figure 1 label #55).

Tissue Viability, Engraftment, and Plexus-To-Plexus Apposition

Neovascularization begins around day 3 of tissue transplant [57,67]. It is robust enough to support most fasciocutaneous flaps by the 12th postoperative day [68]. The periphery of skin flaps derives perfusion from wound bed neo-vessels [57]. Vessels grow at a rate of approximately 0.2 mm per day, continuing up to distances of 2–5 mm [41]. More intervening fat or scar prevents neovascularization. These new vessels are quite small [69,70], and pedicle injury can compromise flaps even years after inset [69,71]. This often complicates fatty abdominal flaps and muscular flaps. Both flaps have barriers to neovascularization (fat and perimysium). Skin flaps undergo revascularization faster than muscle flaps [72]. Skin flaps have large exposed plexi, enabling arteriogenesis

(widening of pre-existing arteries) and angiogenesis (sprouting from existing arteries) before neovascularization (formation of vessels from progenitor cells). Their different perfusion patterns contribute to their differential angiogenesis; skin flaps have an initial vasoconstrictive phase after sympathetic denervation, leading to more hypoxia-signaling, promoting angiogenesis, whereas muscle flaps are less sensitive to denervation, and hypoxia increases perfusion along the pedicle [73]. Supercharging adipose tissue with a dermal plexus flap enhances its viability [74].

Early engraftment enhances the viability of grafts and thin flaps [2,3,4,70,75]. Full-thickness skin grafts (FTSG) may receive dermal plexus perfusion from their margins. Yet, they cannot survive over a poorly perfused bed wider than 12 mm [8,76–78]. Dermal plexus flaps also have a limited zone of perfusion (Table 1) [1], and similarly necrose over poorly perfused beds [6]. Adipose tissue is slippery; engraftment technique is important for composite graft take.

Apposition of the plexi in grafts/flaps and their wound beds improves outcomes [2,79–81]. It leads to inosculation (direct anastomosis) of pre-existing vessels, facilitating engraftment. Graft success may be related to dermal vascular density, which is greater in retroauricular, scalp, thigh, and plantar dermis as compared to the cheek, groin, peri-clavicular, back, and buttock dermis [8]. In the face, extensive communication between angiosomes diminishes the importance of engraftment. Indeed, whole-face transplants and large keystone flaps can be reliably perfused on a single perforator (Figure 2) [82]. Septae between adipocytes contain vessels (Figure 1 label #13). Including the septae in composite grafts thus improves viability [2,46]. Septae are well-defined in the groin, mastoid region, and other anchoring sites (Table 2) [11].

There are different techniques for preserving plexi during dissection. Partial debridement, retaining the deepest, flimsy layer of reticular dermis, maintains the bed's deep dermal plexus (Figure 1 label #11) [2]. To maintain the subdermal plexus in a raised flap/graft, surgeons preserve at least 1 mm of fat during scalpel/scissor dissection [2,83], and 3–5 mm during open-tip liposuction and/or arthroscopic shaving [84,85]. During de-fatting, maintaining the honeycomb fascia helps preserve septal vessels (Figure 1 label #13) [2]. It is very difficult to completely de-fat a pure-skin perforator flap [1,49]. Defatting to less than 1 mm can insult plexi and deep dermal structures, compromising perfusion and contributing to post-inflammatory hyperpigmentation [2,86]. Preserving more than 4 mm of fat limits engraftment [2,87]. The suprafascial plexus is easily maintained by dissecting fat off it [79–81]. In patients with thick fascia, as seen in chronic lymphedema, deep subfascial plexi are made accessible by fascial thinning to 1 mm [75].

Neurotization

Skin neurotization causes vasospasm [72]. Skin sympathetic denervation en-

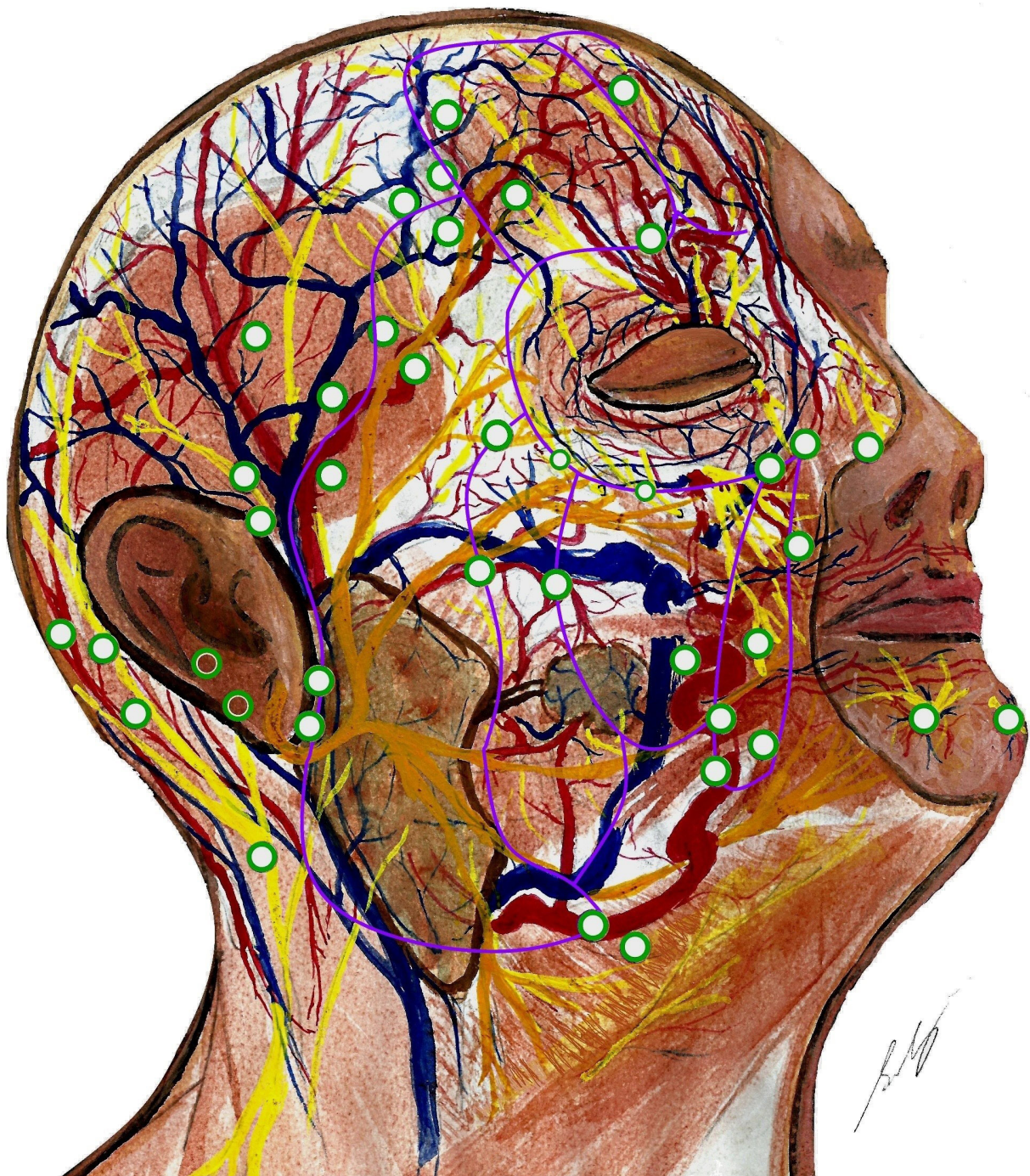


Figure 2. Facial neurovasculature with perforators mapped. Perforators (green) originate where dominant vessels traverse fixed connective tissue planes (purple). Perforators supply the superficial musculoaponeurotic system (SMAS) and the supra-SMAS fat compartments and skin. They are longer in the more mobile lateral face, and shorter and more clustered medially. Perforators often enter SMAS alongside nerves. Veins generally travel apart from arteries in scalp, forehead, and nasolabial regions. The genu (knee) of the supratrochlear artery is shown, as it emerges from corrugator supercilii. The depiction shows the communication between the zygomatic branch of the facial nerve and the infraorbital nerve, which is located superolateral to the alar rim. Dominant arteries (left to right) include occipital artery, posterior auricular artery, superficial temporal artery, frontal branch of superficial temporal artery, supratrochlear artery, facial artery, and mental artery. Some perforators also arise from the transverse facial artery, zygomaticoorbital artery, zygomaticotemporal artery, zygomaticofacial artery, and infraorbital artery. Fascial septae of midface (left to right): lateral cheek septum, medial cheek septum, middle cheek septum, and nasolabial septum. The orbicularis membrane is superior to them. Forehead vessels (left to right): horizontal limb of frontal branch of superficial temporal artery, ascending branches of supraorbital artery (emerging from below supraorbital ligament), supratrochlear artery, paracentral artery and angular artery, central artery and dorsal nasal artery, and central vein. This figure is an original creation by the first author, prepared for this publication.

hances perfusion after a 24–48-hour vasoconstrictive phase [73]. This may support cutaneous flap perfusion. In contrast, muscle flap perfusion is regulated by metabolic demands [72].

Neurotized tissue can achieve near-normal skin sensitivity [47,88–91]. Flap debulking reduces the distance between skin and deeper nerves, improving sensory outcomes [79–81,91,92]. Though a subpapillary nerve plexus may exist, the majority of sensory innervation comes from the dermal nerve trees that ascend with microangiosome arteries [24,29]. Thus, hinged grafts/deep dermal plexus flaps are unlikely to be neurotized except through their bed.

Post-inflammatory Hyperpigmentation

Post-inflammatory hyperpigmentation (PIH) is a morbid complication of free tissue transfers. It is mediated by dermal fibroblasts and sebocytes, which are abundant in the dense reticular dermis (Figure 1 label #9,38) [93–96]. Cells are activated by ischemia, desiccation, and inflammation, resulting from mechanical trauma, inflammatory dermatoses, photodamage, and endogenous metabolic stresses [96–99]. This is the rationale for prophylactically prescribing oral antioxidants (vitamins C and E) and topical moisturizers [47]. Epithelial pigmentation is brown and fades over months. Dermal pigmentation is grey-brown and persists, particularly in dark-skinned people [100]. The ‘melanocyte-migration hypothesis’ for PIH states that inflammatory signals damage the basement membrane, precipitating melanocyte incontinence into the upper dermis [101,102]. This is readily observed in ‘pie-crust’ skin grafts, which retain dyschromic stab-site scars [4]. Recent evidence challenges this, suggesting PIH results from activation of dormant subdermal melanoblasts [103].

Current microanatomical concepts and clinical observations reveal the complex etiopathogenesis of chronic PIH. While further analysis is necessary, this preliminary review offers the following insights into chronic PIH associated with split-thickness skin grafts (STSG), FTSG, skin-fat composite grafts (SFCG), and very thin flaps:

- Grafts retain features of their donor site; groin grafts have been reported to succumb to localized and systemic acanthosis nigricans [104,105]. Forearm STSG and FTSG are both excellent for covering defects from harvesting radial forearm free flaps [106,107]. When used to cover periocular defects, distant FTSG (supraclavicular or inner brachial) were more prone to hypopigmentation than regional FTSG (eyelid or post-auricular) [108].
- Groin SFCG may be more prone to PIH, as compared to other sites [2,45]. Groin SFCG with 3 or more mm of fat are predisposed to ischemia and chronic PIH independent of, or accompanied by, epithelial necrosis [2]. Groin FTSG may be more prone [109], or similarly prone to PIH as compared to other sites [110,111]. Groin STSG may be similarly prone to PIH as compared to other sites [112]. STSG from hair-bearing skin is susceptible to PIH [94,113,114]. Thicker STSG contain many more melanocytes and mediatory cells than thinner STSG [33,34].
- STSG from hair-bearing skin seems less susceptible to PIH than FTSG [83,109–111]. This has been objectively confirmed by colorimetric assessment [83,111]. This is supported by the mediatory role of dermal fibroblasts and sebocytes [93–96]. However, some studies suggest STSG and FTSG from hair-bearing skin have similar PIH rates [115–117].
- Hyperpigmentation is proportional to the degree of donor-site/recipient-site dermal insult, including ischemic insult [97]. When thigh STSG was placed on partially debrided wounds, it was complicated by more hyperpigmentation than thicker back STSG placed on fully debrided wounds [118]. Dermabrasion and partial debridement of scars also cause chronic PIH in subsequently grafted skin [118,119]. Flap debulking by liposuction with arthroscopic shaving is complicated by PIH [86]. Avoiding ischemia by preserving perforators and subdermal plexi during dissection, and using scalpels instead of scissors for removing fat, makes thin flaps less susceptible to PIH and other complications typically associated with grafts [87,120].
- Glabrous grafts (plantar FTSG, thick STSG, and dermal grafts) do not suffer hyperpigmentation as they have very few melanocytes [33]. Thus, they match well with palmar skin [88,113,121–123]. The thick collagen at this

site also reduces contracture recurrence [114,121–123].

- Graft orientation is unlikely to be related to PIH [124].

PIH is occasionally useful to enhance skin pigmentation, such as during flap debulking, although the extent of pigmentation remains unpredictable [79,125]. Exploring the potential of dermal substitutes to mitigate graft-associated PIH could be pursued, particularly in dark-skinned populations [126].

Debulking

The ultimate aim of debulking surgery is to address both cosmetic concerns (contour, scarring, pigmentation, hirsutism) and functional issues (pliability, sensitivity, grip, skin quality, hindrance to wearing clothes/shoes, speech, swallowing, etc.) in a single stage. Radical debulking results in thin dermal-plexus flaps, which is suitable for tasks like degloved wound coverage, lymphedema debulking, and thick flap revision [3,4,75,127]. Excisional debulking and liposuction are common techniques used for debulking. Other techniques include liposuction with arthroscopic shaving, intricate tissue rearrangement, laser procedures, and coverage with regionally expanded tissue [127]. Among these options, liposuction is the least traumatic for the wound bed. However, debulking can be uneven and often requires multiple stages, and a layer of fat must be retained to control bleeding. Fibrosed fat resulting from inflammation or irradiation is challenging to remove using conventional suction methods. For this purpose, open-tip liposuction and arthroscopic shaving are effective, although they come with the risk of pedicle injury [85,127,128]. Liposuction in combination with circumferential tissue rearrangement can be employed for debulking turnover flaps [129,130].

Debulked flaps are usually perfused by their pedicles and the vessels in the wound bed [57,69,131]. The revascularization of the flap involves early proximal flap arteriogenesis and late distal flap angiogenesis [69]. Often, wound bed angiogenesis alone may prove inadequate [68]. To enhance early perfusion from the surrounding skin, the design may incorporate beveled or de-epithelialized wound margins. This design promotes the alignment of skin structures, facilitating inosculation between the remaining vessels of the deep dermal and subdermal plexi [45–47,132].

Head & Neck Melanoma Metastasis

Head and neck melanomas have a 22% higher mortality compared to other regions, suggesting regional differences in anatomy and melanoma behavior [133]. Lymphatics are concentrated in the scalp and lateral neck. Node biopsies in these regions have a higher detection rate than those of the face and ear [134]. However, detection by lymphoscintigraphy and sentinel lymph node biopsy shows poor efficiency in this region compared to others [135]. Low node positivity is a characteristic specific to melanomas with a diameter of >2.0 mm [52,136]. These findings suggest that large head and neck melanomas also metastasize hematogenously [52,136]. Considering the low prognostic value of sentinel node dissection, early surveillance using 3D SPECT/CT (three-dimensional single photon emission computed tomography/computed tomography) or empirical adjuvant therapy might be considered in the future [52,136]. The challenges of operating in this region could impact outcomes.

Injection Depth

The size of injected particles influences cohesivity, fluency, and degradation time. This guides decisions about appropriate injection site and depth [137]. The different densities of dermal collagen layers also impact fluid flow [9]. The thick middle dermis is dense and reflective, dividing fluids injected above and below it.

Superficial dermal injection is performed at angles up to 12 degrees. It requires little pressure, readily forming a wheal and can be confirmed by visualizing the needle outline through ‘tenting’ [138]. It is useful for hydrodissection before partial debridement [39], or for superficial hypoperfusion using epinephrine-local anesthesia for hair transplant, as per our experience. To fill small wrinkles, less-cohesive fillers (e.g., Belotero hyaluronic acid) are injected in this plane, as they are moldable and spread evenly [139]. Microfat grafts are also injected into the superficial dermis by injecting while withdrawing the

needle from pinched-up skin, minimizing the risk of dermal vascular injection and fat embolism [140]. High-cohesivity fillers (e.g., Radiesse calcium hydroxyapatite and Bellafill polymethylmethacrylate) are not used superficially as they form palpable nodules [141]. Using smaller needles at an angle reduces the risk of them backtracking into the superficial plane [141].

Middle dermal injection is painful and requires high pressure. It is used in scalp infiltration with epinephrine-local anesthetic, with the rationale that deeper infiltration tends to track into the loose areolar plane, minimizing the local effect [142].

Deeper injections remain below this dense middle dermis and tumesce the deep-dermal/subcutaneous plane. Epinephrine-local anesthetic infiltrated into this region may constrict the stem of microangiosomes, regulating flow to the more superficial layers [21,40]. Classical subdermal large-diameter fat grafts are relatively under-perfused and are complicated by atrophy, cysts, nodules, and necrosis [140]. Deeper wrinkles are broken by needle subincision and volumized by high-cohesivity fillers [139].

Resolving Surgical 'Paradoxes'

Reviewing microanatomy clarifies seemingly conflicting surgical observations. Engrafting dermal plexus grafts and flaps and improving marginal perfusion through the alignment of beveled dermal surfaces may enhance tissue viability and patient outcomes.

Regarding dermal plexus flaps, which are mostly fat-free, the deep dermal plexus supplies up to about 12 mm from the flap base [1,8,76–78]. Consequently, large dermal plexus flaps are predominantly perfused through engraftment [3–5]. Poor engraftment compromises debulked dermal plexus flaps [6,7]. Treating these flaps as hinged grafts, such as when redraping limbs, proves to be a successful approach [3–5].

Aligning vessels of similar sizes leads to early anastomoses (inosculation). This principle is exploited in plexus-to-plexus apposition techniques, in which plexi from donor and recipient site tissues are approximated. Inosculation is also promoted by increasing the area of marginal plexus-to-plexus apposition, as accomplished in beveled-margin grafts and flaps [45–47,132]. This latter technique is particularly effective in composite grafts from retroauricular skin, as this skin receives predominantly marginal perfusion, and thus, possesses well-developed deep dermal and subdermal plexi [8]. The ability to survive over poorly perfused beds and to be revascularized by inosculation within 24 hours blurs the distinction between beveled-margin retroauricular composite grafts and free flaps. This holds especially true considering both undergo an early vasoconstrictive phase due to sympathetic denervation [73].

CONCLUSION

Microanatomical concepts must inform surgical practice. Understanding dissection planes helps preserve vascular plexi and ensure tissue viability. The relationships between perforators, angiosomes, and surrounding neurovasculature guide flap design. Understanding the limits of microangiosomes and the deep dermal plexus, as well as the absence of the superficial dermal plexus, underscores the significance of engrafting thin primary and debulked flaps. Apposition of plexi within donor and recipient tissues can enhance tissue viability and neurotization. Chronic post-inflammatory hyperpigmentation after free tissue transfer seems to be influenced by tissue ischemia, donor tissue melanocyte density, recipient site trauma, and dermal fibroblast density. Techniques to enhance microsurgical safety are discussed.

ARTICLE INFORMATION

***Correspondence:** Mohammad Suleman Bajwa, MBBS, MD, Department of Plastic and Reconstructive Surgery & Mayo Burn Centre, Mayo Hospital, King Edward Medical University, Hospital Rd, Anarkali Bazaar Lahore, Punjab 54000, Pakistan. Email: suleman97@outlook.com

Received: Jun. 04, 2023; **Accepted:** Jul. 21, 2023; **Published:** Sep. 14, 2023

DOI: [10.24983/scitemed.imj.2023.00174](https://doi.org/10.24983/scitemed.imj.2023.00174)

Disclosure: The manuscript has not been presented or discussed at any scientific meetings, conferences, or seminars related to the topic of the research.

Ethics Approval and Consent to Participate: The study adheres to the ethical principles outlined in the 1964 Helsinki Declaration and its subsequent revisions, or other equivalent ethical standards that may be applicable. These ethical standards govern the use of human subjects in research and ensure that the study is conducted in an ethical and responsible manner. The researchers have taken extensive care to ensure that the study complies with all ethical standards and guidelines to protect the well-being and privacy of the participants.

Funding: This research was funded in part through National Institutes of Health/National Cancer Institute Cancer Center Support Grant P30 CA008748.

Conflict of Interest: In accordance with the ethical standards set forth by the SciTeMed publishing group for the publication of high-quality scientific research, the author(s) of this article declare that there are no financial or other conflicts of interest that could potentially impact the integrity of the research presented. Additionally, the author(s) affirm that this work is solely the intellectual property of the author(s), and no other individuals or entities have substantially contributed to its content or findings.

Copyright © 2023 The Author(s). The article presented here is openly accessible under the terms of the Creative Commons Attribution 4.0 International License (CC-BY). This license grants the right for the material to be used, distributed, and reproduced in any way by anyone, provided that the original author(s), copyright holder(s), and the journal of publication are properly credited and cited as the source of the material. We follow accepted academic practices to ensure that proper credit is given to the original author(s) and the copyright holder(s), and that the original publication in this journal is cited accurately. Any use, distribution, or reproduction of the material must be consistent with the terms and conditions of the CC-BY license, and must not be compiled, distributed, or reproduced in a manner that is inconsistent with these terms and conditions. We encourage the use and dissemination of this material in a manner that respects and acknowledges the intellectual property rights of the original author(s) and copyright holder(s), and the importance of proper citation and attribution in academic publishing.

Publisher Disclaimer: It is imperative to acknowledge that the opinions and statements articulated in this article are the exclusive responsibility of the author(s), and do not necessarily reflect the views or opinions of their affiliated institutions, the publishing house, editors, or other reviewers. Furthermore, the publisher does not endorse or guarantee the accuracy of any statements made by the manufacturer(s) or author(s). These disclaimers emphasize the importance of respecting the author(s)' autonomy and the ability to express their own opinions regarding the subject matter, as well as those readers should exercise their own discretion in understanding the information provided. The position of the author(s) as well as their level of expertise in the subject area must be discerned, while also exercising critical thinking skills to arrive at an independent conclusion. As such, it is essential to approach the information in this article with an open mind and a discerning outlook.

REFERENCES

- Narushima M, Yamasoba T, Iida T, et al. Pure skin perforator flaps: The anatomical vascularity of the superthin flap. *Plast Reconstr Surg* 2018;142(3):351e–360e.
- Jang YC, Burm JS, Cho JY. Skin-fat composite grafts for reconstructing large full-thickness skin defects. *Plast Reconstr Surg* 2023;151(3):635–644.
- Yan H, Gao W, Li Z, et al. The management of degloving injury of lower extremities: Technical refinement and classification. *J Trauma Acute Care Surg* 2013;74(2):604–610.
- Jeng SF, Hsieh CH, Kuo YR, Wei FC. Technical refinement in the management of circumferentially avulsed skin of the leg. *Plast Reconstr Surg* 2004;114(5):1225–1227.
- Hassan K, Chang DW. The Charles procedure as part of the modern armamentarium against lymphedema. *Ann Plast Surg* 2020;85(6):e37–e43.
- Hallock GG. Conventional liposuction-assisted debulking of muscle perforator flaps. *Ann Plast Surg* 2004;53(1):39–43.
- Sharma RK, Tuli P, Makkar SS. Full-thickness skin graft as a one-stage debulking procedure after free flap reconstruction for the lower leg. *Plast Reconstr Surg* 2007;119(7):2330.
- Tomita K, Hosokawa K, Yano K, Takada A, Kubo T, Kikuchi M. Dermal vascularity

of the auricle: Implications for novel composite grafts. *J Plast Reconstr Aesthet Surg* 2009;62(12):1609–1615.

9. Wang Y, Xu R, He W, et al. Three-dimensional histological structures of the human dermis. *Tissue Eng Part C Methods* 2015;21(9):932–944.
10. Wong R, Geyer S, Weninger W, Guimberteau JC, Wong JK. The dynamic anatomy and patterning of skin. *Exp Dermatol* 2016;25(2):92–98.
11. Nakajima H, Imanishi N, Minabe T, Kishi K, Aiso S. Anatomical study of subcutaneous adipofascial tissue: A concept of the protective adipofascial system (pafs) and lubricant adipofascial system (lafas). *Scand J Plast Reconstr Surg Hand Surg* 2004;38(5):261–266.
12. Segura S, Requena L. Anatomy and histology of normal subcutaneous fat, necrosis of adipocytes, and classification of the panniculitides. *Dermatol Clin* 2008;26(4):419–424.
13. Ishida T, Takeuchi K, Hayashi S, et al. Anatomical structure of the subcutaneous tissue on the anterior surface of human thigh. *Okajimas Folia Anat Jpn* 2015;92(1):1–6.
14. Cancelli R, Zulian A, Gentilini D, et al. Molecular and morphologic characterization of superficial- and deep-subcutaneous adipose tissue subdivisions in human obesity. *Obesity (Silver Spring)* 2013;21(12):2562–2570.
15. Lampejo AO, Ghavimi SAA, Hagerling R, Agarwal S, Murfee WL. Lymphatic/blood vessel plasticity: Motivation for a future research area based on present and past observations. *Am J Physiol Heart Circ Physiol* 2023;324(1):H109–H121.
16. Metz D. Neurophysiology of the skin - Functional anatomy of the skin nervous system. *Exp Dermatol* 2001;10(5):365–366.
17. Taylor GI, Palmer JH. The vascular territories (angiosomes) of the body: Experimental study and clinical applications. *Br J Plast Surg* 1987;40(2):113–141.
18. Imanishi N, Nakajima H, Minabe T, Aiso S. Angiographic study of the subdermal plexus: A preliminary report. *Scand J Plast Reconstr Surg Hand Surg* 2000;34(2):113–116.
19. Saint-Cyr M, Wong C, Schaverien M, Mojallal A, Rohrich RJ. The perforasome theory: Vascular anatomy and clinical implications. *Plast Reconstr Surg* 2009;124(5):1529–1544.
20. Taylor GI, Corlett RJ, Dhar SC, Ashton MW. The anatomical (angiosome) and clinical territories of cutaneous perforating arteries: Development of the concept and designing safe flaps. *Plast Reconstr Surg* 2011;127(4):1447–1459.
21. Geyer SH, Nohammer MM, Tinhofer IE, Weninger WJ. The dermal arteries of the human thumb pad. *J Anat* 2013;223(6):603–609.
22. Taylor GI, Chubb DP, Ashton MW. True and ‘choke’ anastomoses between perforator angiosomes: Part I. Anatomical location. *Plast Reconstr Surg* 2013;132(6):1447–1456.
23. Chen Z, Rank E, Meiburger KM, et al. Non-invasive multimodal optical coherence and photoacoustic tomography for human skin imaging. *Sci Rep* 2017;7(1):17975.
24. Tinhofer IE, Zaussinger M, Geyer SH, et al. The dermal arteries in the cutaneous angiosome of the descending genicular artery. *J Anat* 2018;232(6):979–986.
25. Dabiri B, Kampusch S, Geyer SH, et al. High-resolution episcopic imaging for visualization of dermal arteries and nerves of the auricular cymba conchae in humans. *Front Neuroanat* 2020;14:22.
26. Nakamura Y, Takanari K, Nakamura R, et al. Correlation between blood flow, tissue volume and microvessel density in the flap. *Nagoya J Med Sci* 2020;82(2):291–300.
27. Smahel J, Clodius L. The blood vessel system of free human skin grafts. *Plast Reconstr Surg* 1971;47(1):61–66.
28. Pasyk KA, Argenta LC, Hassett C. Quantitative analysis of the thickness of human skin and subcutaneous tissue following controlled expansion with a silicone implant. *Plast Reconstr Surg* 1988;81(4):516–523.
29. Metz D. Neuroanatomy of the skin. In: *Neuroimmunology of the Skin: Basic Science to Clinical Practice*. Edited by Granstein RD, Luger TA. Berlin, Heidelberg: Springer Berlin Heidelberg; 2009: 3–12.
30. Fernandez-Flores A. Regional variations in the histology of the skin. *Am J Dermatopathol* 2015;37(10):737–754.
31. Iyengar B. The melanocyte photosensory system in the human skin. *Springerplus* 2013;2(1):158.
32. Jang YH, Kim SL, Lee JS, et al. Possible existence of melanocytes or melanoblasts in human sebaceous glands. *Ann Dermatol* 2014;26(4):469–473.
33. Szabo G. The regional anatomy of the human integument with special reference to the distribution of hair follicles, sweat glands and melanocytes. *Phil Trans R Soc Lond B* 1967;252:447–485.
34. Hirobe T, Enami H, Nakayama A. The human melanocyte and melanoblast populations per unit area of epidermis in the rete ridge are greater than in the inter-rete ridge. *Int J Cosmet Sci* 2021;43(2):211–217.
35. Bao H, Cao J, Chen M, et al. Biomarkers of aging. *Sci. China Life Sci* 2023;66(5):893–1066.
36. Czekalla C, Schonborn KH, Lademann J, Meinke MC. Noninvasive determination of epidermal and stratum corneum thickness in vivo using two-photon microscopy and optical coherence tomography: Impact of body area, age, and gender. *Skin Pharmacol Physiol* 2019;32(3):142–150.
37. Langer MF, Unglaub F. The normal fibrous skeleton of the hand and changes in Dupuytren's contracture. In: *Collagenase in Dupuytren Disease*. Edited by Pajardi G, Badalamente M, Hurst L. Springer, Cham;2018:17–38.
38. Schaverien MV, Pessa JE, Rohrich RJ. Vascularized membranes determine the anatomical boundaries of the subcutaneous fat compartments. *Plast Reconstr Surg* 2009;123(2):695–700.
39. Bennett KG, Gilman RH. Intradermal infiltration of local anesthetic—rapid and bloodless deepithelialization of the breast pedicle. *Plast Reconstr Surg Glob Open* 2017;5(2):e1225.
40. Bajwa MS, Bashir MM, Bajwa MH, et al. Local infiltration anesthesia: How best to wait? – A systematic review. *BJs Open* 2023; in press.
41. Hom DB, Goding GS. Skin flap physiology. In: *Local Flaps in Facial Reconstruction*. 2nd ed. Edited by Baker SR. Philadelphia PA: Mosby;2007:15–30.
42. Paul SP. Biodynamic excisional skin tension lines for surgical excisions: Untangling the science. *Ann R Coll Surg Engl* 2018;100(4):330–337.
43. Lucas JB. The physiology and biomechanics of skin flaps. *Facial Plast Surg Clin North Am* 2017;25(3):303–311.
44. Tavis MJ, Thornton JW, Harney JH, Woodroof EA, Bartlett RH. Graft adherence to de-epithelialized surfaces: A comparative study. *Ann Surg* 1976;184(5):594–600.
45. Burm JS. Reconstruction of the nasal tip including the columella and soft triangle using a mastoid composite graft. *J Plast Reconstr Aesthet Surg* 2006;59(3):253–256.
46. Burm JS, Hansen JE. Full-thickness skin grafting with marginal deepithelialization of the defect for reconstruction of helical rim keloids. *Ann Plast Surg* 2010;65(2):193–196.
47. Lee JH, Burm JS, Kang SY, Yang WY. Full-thickness skin grafting with de-epithelialization of the wound margin for finger defects with bone or tendon exposure. *Arch Plast Surg* 2015;42(3):334–340.
48. Morris M, Schreiber MA, Ham B. Novel management of closed degloving injuries. *J Trauma* 2009;67(4):E121–123.
49. Kwon JG, Brown E, Suh HP, Pak CJ, Hong JP. Planes for perforator/skin flap elevation-definition, classification, and techniques. *J Reconstr Microsurg* 2023;39(3):179–186.
50. Cracowski JL, Roustit M. Human skin microcirculation. *Compr Physiol* 2020;10(3):1105–1154.
51. Zerbino DD, Gavriash AS. [Transformation in the lymphatic system of the heart and myocardium in congestion with lymph]. *Arkh Patol* 1975;37(10):30–35.
52. Fadaki N, Li R, Parrett B, et al. Is head and neck melanoma different from trunk and extremity melanomas with respect to sentinel lymph node status and clinical outcome? *Ann Surg Oncol* 2013;20(9):3089–3097.
53. Pan WR, Le Roux CM, Briggs CA. Variations in the lymphatic drainage pattern of the head and neck: Further anatomic studies and clinical implications. *Plast Reconstr Surg* 2011;127(2):611–620.
54. Shoukath S, Taylor GI, Mendelson BC, et al. The lymphatic anatomy of the lower eyelid and conjunctiva and correlation with postoperative chemosis and edema. *Plast Reconstr Surg* 2017;139(3):628e–637e.
55. Slavin SA, Upton J, Kaplan WD, Van den Abbeele AD. An investigation of lymphatic function following free-tissue transfer. *Plast Reconstr Surg* 1997;99(3):730–741; discussion 742–733.
56. Gascoigne AC, Ian Taylor G, Corlett RJ, Briggs C, Ashton MW. The relationship of superficial cutaneous nerves and interperforator connections in the leg: A cadaveric anatomical study. *Plast Reconstr Surg* 2017;139(4):994e–1002e.
57. Tsur H, Daniller A, Strauch B. Neovascularization of skin flaps: Route and timing. *Plast Reconstr Surg* 1980;66(1):85–90.
58. D'Arpa S, Pirrello R, Toia F, Moschella F, Cordova A. Reconstruction of nasal alar defects with freestyle facial artery perforator flaps. *Facial Plast Surg* 2014;30(3):277–286.
59. Qassemayr Q, Havet E, Sinna R. Vascular basis of the facial artery perforator flap: Analysis of 101 perforator territories. *Plast Reconstr Surg* 2012;129(2):421–429.
60. Houseman ND, Taylor GI, Pan WR. The angiosomes of the head and neck: Anatomical study and clinical applications. *Plast Reconstr Surg* 2000;105(7):2287–2313.
61. Taylor GI, Caddy CM, Watterson PA, Crock JG. The venous territories (venosomes) of the human body: Experimental study and clinical implications. *Plast Reconstr Surg* 1990;86(2):185–213.
62. Koziej M, Polak J, Holda J, et al. The arteries of the central forehead: Implications for facial plastic surgery. *Aesthet Surg J* 2020;40(10):1043–1050.
63. Stigall LE, Bramlette TB, Zitelli JA, Brodland DG. The paramidline forehead flap: A clinical and microanatomic study. *Dermatol Surg* 2016;42(6):764–771.
64. Kleintjes WG. Forehead anatomy: Arterial variations and venous link of the midline forehead flap. *J Plast Reconstr Aesthet Surg* 2007;60(6):593–606.
65. Tansatit T, Phanchart P, Chinnawong D, Apinuntrum P, Phetudom T, Sahraoui YM. A cadaveric study of the communication patterns between the buccal trunks of the

facial nerve and the infraorbital nerve in the midface. *J Craniofac Surg* 2016;27(1):214–218.

66. Southwood WF. The thickness of the skin. *Plast Reconstr Surg (1946)* 1955;15(5):423–429.

67. Clemmesen T, Ronhovde DA. Restoration of the blood-supply to human skin autografts. *Scand J Plast Reconstr Surg* 1968;2(1):44–46.

68. Yoon AP, Jones NF. Critical time for neovascularization/angiogenesis to allow free flap survival after delayed postoperative anastomotic compromise without surgical intervention: A review of the literature. *Microsurgery* 2016;36(7):604–612.

69. Kumar K, Jaffe W, London NJ, Varma SK. Free flap neovascularization: Myth or reality? *J Reconstr Microsurg* 2004;20(1):31–34.

70. McGuire PG, Howdieshell TR. The importance of engraftment in flap revascularization: Confirmation by laser speckle perfusion imaging. *J Surg Res* 2010;164(1):e201–212.

71. Longo B, Laporta R, Sorotos M, Atzeni M, Santanelli di Pompeo F. Complete diep flap survival following pedicle resection, 4 years after its transfer. Clinical evidence of autonomization. *Case Reports Plast Surg Hand Surg* 2016;3(1):70–72.

72. Nasir S, Baykal B, Altuntas S, Aydin MA. Hemodynamic differences in blood flow between free skin and muscles flaps: Prospective study. *J Reconstr Microsurg* 2009;25(6):355–360.

73. Jurell G. Adrenergic nerves and the delay phenomenon. *Ann Plast Surg* 1986;17(6):493–497.

74. Yoshikawa M, Ishitobi M, Matsuda S, et al. A new indication and surgical procedure to reduce fat necrosis after breast-conserving surgery using an inframammary adipofascial flap. *Asian J Surg* 2022;45(11):2268–2272.

75. Chen SH, Cem Yildirim ME, Mousavi SA, Chen HC. Long-term functional outcomes upon application of split-thickness skin graft around major joints in HCC (Hung-Chi Chen)-modified Charles' procedure for advanced lymphedema. *Asian J Surg* 2021;44(1):169–173.

76. Rees TD, Ballantyne DJ, Hawthorne GA, Nathan A. Effects of silastic sheet implants under simultaneous skin autografts in rats. *Plast reconstr surg* 1968;42(4):339–342.

77. Gingrass P, Grabb WC, Gingrass RP. Skin graft survival on avascular defects. *Plast Reconstr Surg* 1975;55(1):65–70.

78. Wright JK, Brawer MK. Survival of full-thickness skin grafts over avascular defects. *Plast Reconstr Surg* 1980;66(3):428–432.

79. Lin TS, Jeng SF, Chiang YC. Resurfacing with full-thickness skin graft after debulking procedure for bulky flap of the hand. *J Trauma* 2008;65(1):123–126.

80. Lin TS. One-stage debulking procedure after flap reconstruction for degloving injury of the hand. *J Plast Reconstr Aesthet Surg* 2016;69(5):646–651.

81. Jaramillo Del Rio AE, Hsieh MH, Kuo PJ, Lin TS. Optimal result of one-stage secondary debulking procedure after flap reconstruction of the ankle. *Ann Plast Surg* 2019;82(5):560–564.

82. Gunnarsson GL, Jackson IT, Thomsen JB. Freestyle facial perforator flaps—a safe reconstructive option for moderate-sized facial defects. *Eur J Plast Surg* 2014;37(6):315–318.

83. Kim TG, Choi MK. Secondary contouring of flaps. *Arch Plast Surg* 2018;45(4):319–324.

84. Ibrahim AE, Janom H, Raad M. Liposuction contouring after head and neck free flap reconstruction. *Anaplastology* 2015;4(2):145.

85. Lai HT, Kuo PJ, Chang CH, Lai CS, Lin SD, Kuo YR. Combined use of liposuction and arthroscopic shaving for delayed debulking of free flaps in head and neck reconstruction. *Ann Plast Surg* 2018;80(2S Suppl 1):S36–S39.

86. Ooi A, Wong CH, Ong YS. Combined use of liposuction and arthroscopic shaver in lower-limb fasciocutaneous flap contouring. *J Plast Reconstr Aesthet Surg* 2013;66(4):538–542.

87. Zhou ZB, Pan D, Wu PF, et al. Utilization of microdissected thin perforator flap technique in the treatment of bulky and deformed skin flaps. *Ann Plast Surg* 2018;80(6):634–638.

88. Wu LC, Gottlieb LJ. Glabrous dermal grafting: A 12-year experience with the functional and aesthetic restoration of palmar and plantar skin defects. *Plast Reconstr Surg* 2005;116(6):1679–1685.

89. Cornelissen AJM, van Onna MA, Keuter XHA, van der Hulst RR. Innervated full thickness grafts in distal finger amputations. *Chin J Traumatol* 2017;20(6):355–358.

90. Inbal R, Rouso M, Ashur H, Wall PD, Devor M. Collateral sprouting in skin and sensory recovery after nerve injury in man. *Pain* 1987;28(2):141–154.

91. Nakamura K, Namba K, Tsuchida H. A retrospective study of thick split-thickness plantar skin grafts to resurface the palm. *Ann Plast Surg* 1984;12(6):508–513.

92. Li Z, Luan J. Long-term results of a one-stage secondary debulking procedure after flap reconstruction for foot. *Plast Reconstr Surg* 2017;139(2):578e–579e.

93. Flori E, Mastrofrancesco A, Mosca S, et al. Sebocytes contribute to melasma onset. *iScience* 2022;25(3):103871.

94. MacNeil S. Progress and opportunities for tissue-engineered skin. *Nature* 2007;445(7130):874–880.

95. Duval C, Cohen C, Chagnoleau C, Flouret V, Bourreau E, Bernerd F. Key regulatory role of dermal fibroblasts in pigmentation as demonstrated using a reconstructed skin model: Impact of photo-aging. *PLoS One* 2014;9(12):e114182.

96. Yuan XH, Jin ZH. Paracrine regulation of melanogenesis. *Br J Dermatol* 2018;178(3):632–639.

97. Taylor S, Grimes P, Lim J, Im S, Lui H. Postinflammatory hyperpigmentation. *J Cutan Med Surg* 2009;13(4):183–191.

98. Vachiramam V, Thadanipon K. Postinflammatory hypopigmentation. *Clin Exp Dermatol* 2011;36(7):708–714.

99. Upadhyay PR, Ho T, Abdel-Malek ZA. Participation of keratinocyte- and fibroblast-derived factors in melanocyte homeostasis, the response to uv, and pigmentary disorders. *Pigment Cell Melanoma Res* 2021;34(4):762–776.

100. Lee AY. Skin pigmentation abnormalities and their possible relationship with skin aging. *Int J Mol Sci* 2021;22(7).

101. Nieuweboer-Krobotova L. Hyperpigmentation: Types, diagnostics and targeted treatment options. *J Eur Acad Dermatol Venereol* 2013;27 Suppl 1:2–4.

102. Lacz NL, Vafaie J, Kihiczak NI, Schwartz RA. Postinflammatory hyperpigmentation: A common but troubling condition. *Int J Dermatol* 2004;43(5):362–365.

103. Cramer SF, Salgado CM, Reyes-Mugica M. A study of dermal melanophages in childhood nevi. Reassessing so-called “pigment incontinence”. *J Cutan Pathol* 2020;47(9):809–814.

104. Wu JC, Cunningham BB. Ectopic acanthosis nigricans occurring in a child after syndactyly repair. *Cutis* 2008;81(1):22–24.

105. Burke E, DeCoste RC, Wright GR, Fraser RB, Walsh NM, Bezuhly M. “Ectopic acanthosis nigricans” in inguinal skin grafted to the hands of a child. *JAAD Case Rep* 2022;27:3–5.

106. Vahldieck M, Zyba V, Hartwig S, Passmann B, Scheer M. Retrospective comparison of split-thickness skin graft versus local full-thickness skin graft coverage of radial forearm free flap donor site. *J Craniomaxillofac Surg* 2022;50(8):664–670.

107. Kajikawa A, Ueda K, Katsuragi Y. Split-thickness skin flap technique for elevating the radial forearm flap. *Plast Reconstr Surg* 2009;123(1):284–287.

108. Rathore DS, Chickadasarahilli S, Crossman R, Mehta P, Ahluwalia HS. Full thickness skin grafts in periorcular reconstructions: Long-term outcomes. *Ophthalmic Plast Reconstr Surg* 2014;30(6):517–520.

109. Paterson P, Titley OG, Nancarrow JD. Donor finger morbidity in cross-finger flaps. *Injury* 2000;31(4):215–218.

110. Deunk J, Nicolai JP, Hamburg SM. Long-term results of syndactyly correction: Full-thickness versus split-thickness skin grafts. *J Hand Surg Br* 2003;28(2):125–130.

111. Elrod J, Moellmeier D, Schiestl C, Mohr C, Neuhaus K. Comparative analysis of functional and aesthetic outcomes of retroauricular full thickness versus plantar glabrous split thickness skin grafts in pediatric palmar hand burns. *Burns* 2020;46(3):639–646.

112. Eryilmaz T, Tellioglu AT, Ozakpinar HR, et al. Correction of hyperpigmented palmar grafts with full-thickness skin grafts from the lateral aspect of the foot. *J Plast Surg Hand Surg* 2013;47(5):405–408.

113. Moon SH, Lee SY, Jung SN, et al. Use of split thickness plantar skin grafts in the treatment of hyperpigmented skin-grafted fingers and palms in previously burned patients. *Burns* 2011;37(4):714–720.

114. Marques RR, Coltro PS, Almeida JB, Castro JCD, Junior JAF. Treating complex palmar-plantar wounds using a bilaminar ‘trapdoor’ technique: A case series. *J Wound Care* 2021;30(10):868–873.

115. Chan QE, Barzi F, Harvey JG, Holland AJ. Functional and cosmetic outcome of full-versus split-thickness skin grafts in pediatric palmar surface burns: A prospective, independent evaluation. *J Burn Care Res* 2013;34(2):232–236.

116. Al-Qattan MM. Campfire burns of the palms in crawling infants in Saudi Arabia: Results following release and graft of contractures. *J Burn Care Res* 2009;30(4):616–619.

117. Schwanholt C, Greenhalgh DG, Warden GD. A comparison of full-thickness versus split-thickness autografts for the coverage of deep palm burns in the very young pediatric patient. *J Burn Care Rehabil* 1993;14(1):29–33.

118. Kubota Y, Mitsukawa N, Chuma K, et al. Hyperpigmentation after surgery for a deep dermal burn of the dorsum of the hand: Partial-thickness debridement followed by medium split-thickness skin grafting vs full-thickness debridement followed by thick split-thickness skin grafting. *Burns Trauma* 2016;4:9.

119. Harmon CB, Skinner DP. Dermabrasion. In: *Cosmetic Dermatology: Products and Procedures*. 3rd ed. Edited by Draeos ZD. John Wiley & Sons Ltd;2022:547–554.

120. Yamamoto T, Yamamoto N, Fuse Y, Kageyama T, Sakai H, Tsukuura R. Subdermal dissection for elevation of pure skin perforator flaps and superthin flaps: The dermis as a landmark for the most superficial dissection plane. *Plast Reconstr Surg* 2021;147(3):470–478.

121. Sohail M, Hussain M, Bashir MM, et al. Outcome of coverage of post burn palmar hand contractures with glabrous intermediate-thickness plantar (ITP) skin graft. *Ann*

- King Edw Med Univ* 2017;23:3.
122. Friel MT, Duquette SP, Ranganath B, Burkey BA, Glat PM, Davis WJ, 3rd. The use of glabrous skins grafts in the treatment of pediatric palmar hand burns. *Ann Plast Surg* 2015;75(2):153–157.
 123. Jiang Y, Guo R, Zhou S, Wang B, Sun W. Functional and aesthetic reconstruction of digital flexion contractures with full-thickness plantar skin grafts in children. *Dermatol Ther* 2020;33(6):e14466.
 124. Motamedolshariati M, Rezaei E, Shakeri MS, Beiraghi-Toosi A. Does orientation of full-thickness groin grafts affect hyperpigmentation in burn contracture and syndactyly hands? *World J Plast Surg* 2014;3(1):35–36.
 125. Agrawal K, Agrawal A. Vitiligo: Repigmentation with dermabrasion and thin split-thickness skin graft. *Dermatol Surg* 1995;21(4):295–300.
 126. Watfa W, di Summa PG, Meuli J, Raffoul W, Bauquis O. Matriderm decreases donor site morbidity after radial forearm free flap harvest in transgender surgery. *J Sex Med* 2017;14(10):1277–1284.
 127. Nelson JA, Fischer JP, Haddock NT, et al. Striving for normalcy after lower extremity reconstruction with free tissue: The role of secondary esthetic refinements. *J Reconstr Microsurg* 2016;32(2):101–108.
 128. Hallock GG. Defatting of flaps by means of suction-assisted lipectomy. *Plast Reconstr Surg* 1985;76(6):948–952.
 129. Huang SH, Wu SH, Chang KP, et al. Contour refinements of free flaps for optimal outcome in oral reconstruction: Combination of modified liposuction technique and w-plasty in one-stage procedure. *J Craniomaxillofac Surg* 2009;37(4):201–205.
 130. Chang KP, Lai CS, Lin SD. Recontouring commissuroplasty after reconstruction of large defects after resections for head and neck cancer with commissure involvement using an anterolateral thigh flap. *Scand J Plast Reconstr Surg Hand Surg* 2009;43(5):256–259.
 131. Bui DT, Mehrara BJ, Disa JJ, Cordeiro PG. Use of liposuction for secondary revision of irradiated and nonirradiated free flaps. *Ann Plast Surg* 2004;52(6):541–545.
 132. Feinendegen DL, Grubnik A, Feinendegen SY. An algorithm for prevention of unsightly facial scars considering the newest research insights. *Plast Reconstr Surg Glob Open* 2022;10(11):e4635.
 133. Cabrera CI, Li S, Conic R, Gastman BR. The national cancer database: Survival between head and neck melanoma and melanoma of other regions. *Otolaryngol Head Neck Surg* 2022;167(2):286–297.
 134. Parrett BM, Kashani-Sabet M, Singer MI, et al. Long-term prognosis and significance of the sentinel lymph node in head and neck melanoma. *Otolaryngol Head Neck Surg* 2012;147(4):699–706.
 135. Zhang Y, Liu C, Wang Z, et al. Sentinel lymph node biopsy in head and neck cutaneous melanomas: A prisma-compliant systematic review and meta-analysis. *Medicine (Baltimore)* 2021;100(5):e24284.
 136. Carlson GW, Murray DR, Lyles RH, Hestley A, Cohen C. Sentinel lymph node biopsy in the management of cutaneous head and neck melanoma. *Plast Reconstr Surg* 2005;115(3):721–728.
 137. Herrmann JL, Hoffmann RK, Ward CE, Schulman JM, Grekin RC. Biochemistry, physiology, and tissue interactions of contemporary biodegradable injectable dermal fillers. *Dermatol Surg* 2018;44 Suppl 1:S19–S31.
 138. Micheels P, Sarazin D, Besse S, Sundaram H, Flynn TC. A blanching technique for intradermal injection of the hyaluronic acid belotero. *Plast Reconstr Surg* 2013;132(4 Suppl 2):595–685.
 139. Pierre S, Liew S, Bernardin A. Basics of dermal filler rheology. *Dermatol Surg* 2015;41 Suppl 1:S120–126.
 140. Zeltzer AA, Tonnard PL, Verpaele AM. Sharp-needle intradermal fat grafting (snif). *Aesthet Surg J* 2012;32(5):554–561.
 141. Lee JC, Lorenc ZP. Synthetic fillers for facial rejuvenation. *Clin Plast Surg* 2016;43(3):497–503.
 142. Na YC, Park R, Jeong HS, Park JH. Epinephrine vasoconstriction effect time in the scalp differs according to injection site and concentration. *Dermatol Surg* 2016;42(9):1054–1060.